3. Scanning BRILLOUIN microscopy

3.1. Principles of scanning BRILLOUIN microscopy versus ultrasonic pulse-echo techniques

Acoustic microscopy spatially resolves the variation of acoustic properties of matter in order to get information about its morphology. The maximal spatial resolution is roughly given by the wavelength of the acoustic probe. For ultrasonic techniques the term 'acoustic properties' is often related to the specific acoustic impedance Z_a (unit: rayl), according to:

$$Z_a(\vec{r}) = \sqrt{\rho(\vec{r}) \cdot c_{ii}(\vec{q},\vec{r})} = \rho(\vec{r}) \cdot v(\vec{q},\vec{r}), \text{ with } i = 1, 2, ..., 6 , \quad (3.1)$$

where $\vec{q}$ denotes here a unit wave vector directed along a pure mode direction of an anisotropic material, $\vec{r}$ the position vector related to the sample coordinate system and c_{ii} the involved elastic modulus (AULD 1973, MAEV 2008, BRIGGS & KOLOSOV 2009). This relation bases on the assumption that the sample predominantly behaves elastically at the probe frequency and that the approximation of pure acoustic mode wave propagation is valid. The sample's morphology is usually mapped by measuring the relative changes of the specific acoustic impedance $Z_a(\vec{r})$ for a suitable set of position vectors $\{\vec{r}\}$ (LEVIN *et al.* 1988, MAEV *et al.* 2002, MAEV 2008, BRIGGS & KOLOSOV 2009). The mapping of acoustic properties is a common feature of ultrasonic pulse echo-techniques and scanning BRILLOUIN microscopy (SBM). Apart from that, the working principles of both techniques and the probed properties differ significantly, as listed below:

i.) For SBM optically transparent or translucent samples are needed in order to access the bulk acoustic properties. Else in essence only surface acoustic waves can be probed.

ii.) SBM usually explores thermally excited acoustic modes. In contrast to pulse-echo techniques it does not need external sound excitation e.g. by electro-acoustic transducers.

iii.) SBM is hardly limited by hypersonic attenuation, on the contrary to pulse-echo techniques measuring in the GHz regime. In many cases the sensitivity of

pulse-echo techniques is even insufficient for investigations of soft matter probed at GHz frequencies.

iv.) In contrast to pulse-echo methods, SBM measures absolute values of acoustic properties and not only relative ones. However, the absolute values of hypersonic properties derived from SBM data can often only be exactly calculated if the sample's refractive index is known (see section 2.3).

v.) Whereas the pulse-echo method presets the sound frequency in combination with the direction of wave propagation within the sample, SBM presets the direction and the norm of the acoustic wave vector. The possibility to select the wave vector $\vec{q}$ during SBM allows the experimentalist probing elastic anisotropy and acoustic dispersion by adjusting either the direction or the norm of $\vec{q}$. Hence, for an acoustic map recorded by SBM, the hypersonic velocity and attenuation can be indicated for each scattering volume in dependence of both the direction and norm of the wave vector $\vec{q}$.

vi.) Another important difference between both techniques concerns the number of probed acoustic modes in one data record. Whereas pulse-echo techniques need two separate transducers to excite and probe the longitudinally and transversely polarized sound modes, SBM records simultaneously within one BRILLOUIN spectrum the properties of the three thermally excited phonon modes present in the homogeneous scattering volume. In other words, for SBM every BRILLOUIN spectrum directly yields the hypersonic properties for the complete set of eigenmodes for a given wave vector $\vec{q}(\vec{r})$, provided the opto-acoustic coupling is sufficiently high (VACHER & BOYER 1972).

vii.) The lateral dimensions of the scattering volume realised in SBM are usually in between 1 and 30 microns. The corresponding scattering volumes range between 10^{-18} m^3 and 10^{-14} m^3, respectively.

In the following the common BRILLOUIN microscopy setups discussed in literature are classified within two main groups regarding the used scattering geometry: SBM^{180}, making use of the backscattering geometry and $SBM^{\theta A}$, employing the

θA scattering geometry. The differences of the working principles, the experimental realization and the accessed information are delineated below.

3.2. Confocal scanning BRILLOUIN microscopy and other SBM techniques using backscattering

Inspired by confocal RAMAN microscopy (TURRELL & CORSET 1996, GEORGE 2003), several research groups have developed prototypes for confocal BRILLOUIN microscopy working in backscattering geometry with typical scattering volumes of minimal 10^{-18} m^3 (e.g. TAKAGI & KURIHARA 1992, AHART *et al.* 1996, ZHA *et al.* 1996, AHART *et al.* 1999, JIANG & KOJIMA 2000, DEMIDOV *et al.* 2004, KIM *et al.* 2005, PERZLMAIER *et al.* 2005, BRETOS *et al.* 2007, SAKAMOTO *et al.* 2008, SANDWEG *et al.* 2008, SVANIDZE *et al*. 2009, HASHIMOTO *et al.* 2010, JIMÉNEZ RIOBÓO *et al.* 2010). Since commercially available optical microscopes can be employed for focusing the incident laser beam on the sample and collecting the inelastically scattered light, this SBM^{180} setup is nowadays the most frequently applied. The fast assembling of the microscope in the outer spectrometer setup and the comparably easy handling are more technical advantages of this powerful experimental technique.

Figure 3.1 gives a schematic view of the SBM^{180} technique including the sample, the incident and the scattered light paths, while omitting the pinholes responsible for confocality as well as the magnifying optics. The sample can be scanned along the three directions $\vec{z}_1$, $\vec{z}_2$ and $\vec{z}_3$, while $\vec{q}^{180}(\vec{r})$ is directed along the $\vec{z}_3$ direction (see section 2.3). Because of the small focal length of the objective lens of the microscope (of typically a few millimetres), the z_3-scanning range within the sample is very limited. Remember that generally the backscattering geometry does not allow the detection of purely transversely polarized modes (VACHER & BOYER 1972). Hence shear modes cannot be probed in isotropic matter using SBM^{180}.

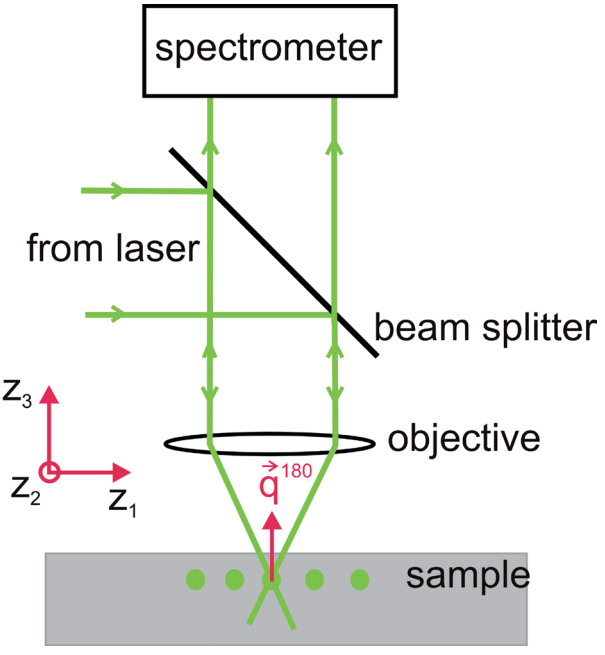

Fig. 3.1. Cursory schematic drawing of a confocal SBM^{180} setup. $\vec{q}^{180}$: wave vector of the probed acoustic phonon. The pinholes responsible for the confocality as well as the magnifying optics are omitted (see e.g. GEORGE 2003). Green dots: sampling laser beam of confocal SBM^{180}.

A different experimental approach consists in designing a backscattering setup based on focusing and collecting optics having a much larger focal distance, e.g. of 100 mm (PHILIPP *et al.* 2009, 2011, SANCTUARY *et al.* 2010). Such a setup, schematically indicated in figure 3.2, permits a high two-dimensional spatial resolution in the (z_1, z_2)-plane and a low resolution in the z_3-direction. That's why we call this backscattering setup in the following SBM^{180-2D}. The drawback of the low resolution in the z_3-direction is partially compensated by the fact that if multiple phonon doublets of longitudinally polarized acoustic modes are recorded within one BRILLOUIN spectrum, then this is indicative for elastic heterogeneities within the scattering volume (SANCTUARY *et al.* 2010, PHILIPP *et al.* 2011). The comparatively large scattering volume leads of course to a higher number of

inelastically scattered photons so that the solid angle of phonon wave vectors can be in most cases much more limited than for confocal scanning BRILLOUIN microscopy. Furthermore, the comparably large information volume allows for a high temporal resolution as BRILLOUIN spectra can be recorded faster than in other common scattering geometries. During the last years, the SBM^{180-2D} technique has proved to be especially suitable for studying the time evolution of processes occurring within minutes to weeks within isotropic, but inhomogeneous or heterogeneous matter by scanning in the z_1- and z_2-direction (PHILIPP *et al.* 2009, 2011, SANCTUARY *et al.* 2009, 2010).

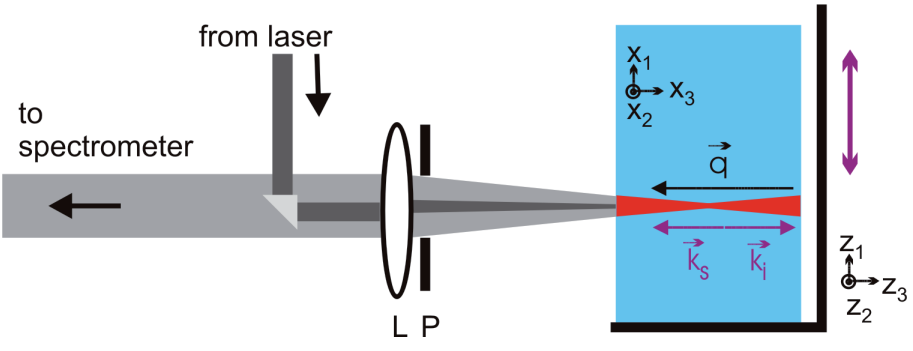

Fig. 3.2. Schematic drawing of the SBM^{180-2D} setup. Sample marked in blue, scattering volume marked in red, L: lens, P: pinhole, $\{x_1, x_2, x_3\}$: sample coordinate system, $\{z_1, z_2, z_3\}$: laboratory coordinate system. Magenta arrow indicating the most commonly utilized scanning direction z_1.

3.2.1 Some drawbacks of the backscattering setup

Beside the aforementioned worth of these SBM techniques using backscattering geometry, they have some inherent drawbacks as stated e.g. by TAKAGI & KURIHARA (1992). A serious drawback of the backscattering technique for SBM investigations consists in the fixed orientation of the phonon wave vector $\vec{q}^{180}$. An instructive example delineated below is the probing of microwave-induced

hypersonic waves by SBM. The technological relevance of induced sound waves is elucidated in section 4.1. As depicted in figure 3.3, a longitudinally polarized surface acoustic wave field initially propagating purely along the $\vec{x}_1$-direction of the sample is excited by a piezoelectric transducer. Its wave vector $\vec{q}(\vec{r})$ is hence parallel to $\vec{x}_1$. The surface acoustic wave field can be characterized on the sample's upper (x_1, x_2)-surface by probing thereon the hypersonic properties. At first sight, the confocal backscattering setup depicted in figure 3.1 seems adequate for this study. But note that this backscattering setup only allows probing phonon wave vectors oriented along $\vec{x}_3$, but not along $\vec{x}_1$ on the (x_1, x_2)-surface! Rotating the sample by 90° around the $\vec{z}_2$-axis does not solve the problem as in that case no spatial resolution of the hypersonic properties in the $\vec{x}_1$-direction can be achieved. Hence, the backscattering geometry is inherently unsuitable for probing the induced surface acoustic wave field. In section 4.1 we illustrate how the θA scattering geometry permits to solve this problem.

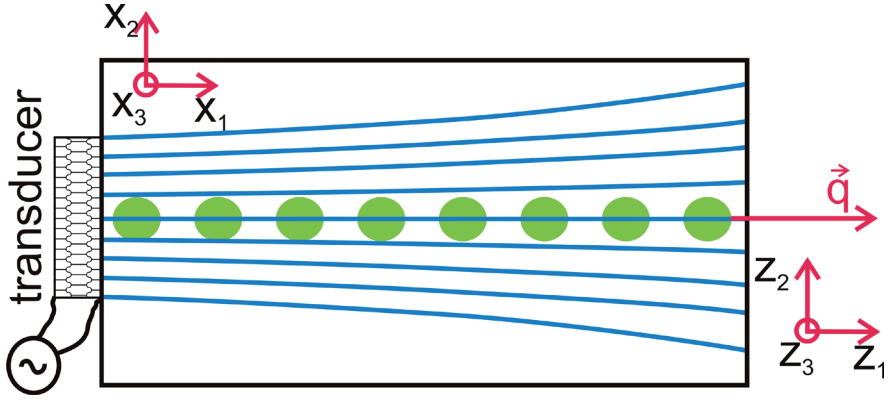

Fig. 3.3. Schematic drawing of an acoustic field induced by a transducer within a rectangular sample. The blue lines represent the acoustic field of microwave-induced acoustic waves with wave vector $\vec{q}$ propagating predominantly along $\vec{x}_1$ within the sample. Green spots: sampling laser beam. $\{z_1, z_2, z_3\}$: laboratory coordinate system, $\{x_1, x_2, x_3\}$: sample coordinate system.

Another drawback stems from the important $\vec{q}$-dependence of the acoustic phonon frequencies. This dependency results from the considerable dispersion of acoustic modes, in contrast to the optical modes probed by RAMAN microscopy (KITTEL 2005). In case of SBM[180], the short working distance of commercial microscope objectives of typically a few millimetres implies that a large solid angle of scattered light is collected. The associated large angle dispersion of $\vec{q}$ strongly broadens the BRILLOUIN lines, thus obscuring all information about sound attenuation and rendering the sound velocity determination uncertain. Note that for anisotropic samples this important $\vec{q}$-dependence leads in addition to an asymmetrical deformation of the BRILLOUIN lines.

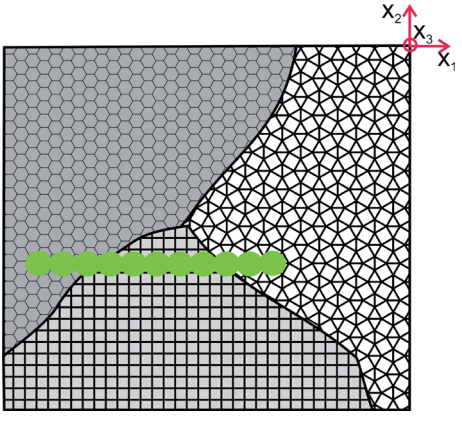

Fig. 3.4. Schematic representation of a polycrystalline sample consisting of grains (or domains) with varying material properties and differently oriented symmetry coordinate systems $\{y_1, y_2, y_3\}$ (not shown in the figure). Sample coordinate system $\{x_1, x_2, x_3\}$. Green spots: trace of the scattering volumes passing through the three grains.

Furthermore, for anisotropic samples scanning BRILLOUIN microscopy performed in backscattering geometry cannot distinguish whether a spatial change in sound velocity is due to a space-dependent material composition or due to differently oriented crystal grains or domains within the same sample. This drawback bases on the refractive index-dependence of the phonon wave vector and

the incapacity of measuring purely transversely polarized acoustic modes in backscattering geometry. In figure 3.4 is depicted such a polycrystalline material, which grains with varying material properties have differently oriented symmetry coordinate systems. In literature the acoustic properties of polycrystalline materials are sometimes probed by means of confocal SBM^{180} while selecting a fixed direction of the phonon wave vector $\vec{q}^{180}(\vec{r})$ parallel to $\vec{x}_3$ and by scanning the sample's properties in the (x_1, x_2)-plane. However, scanning BRILLOUIN microscopy performed in backscattering geometry cannot discriminate whether the BRILLOUIN features recorded for instance on the trace given by the green spots in figure 3.4 stem from changed grain orientations of grains made of the same material or rather from a varying material composition of the grains. In addition, the elastic tensor of the different grains cannot be calculated using SBM^{180}. The combination of SBM with the θA scattering technique, $SBM^{\theta A}$, helps to overcome this inherent problem. In this context, two illustrative examples for the determination of the elastic properties of polycrystalline films are given in chapter 4.

3.3. An alternative scanning BRILLOUIN microscopic technique

An alternative SBM technique (SANCTUARY *et al.* 2003) uses the θA scattering geometry (see section 2.3); because of its easy alignment the 90A scattering geometry is chosen in many cases. As shown in figure 3.5, $SBM^{\theta A}$ possesses an intermediate imaging system (D1-L2-P1) which maps the scattering volume $V(\vec{r})$ located within the sample to the pinhole P1 of the real microscope. The aim of this intermediate imaging system is fourfold: first, it provides a moderate magnification of the object, second a spatial filtering of the scattering volume selected for the spectral information, third it reproduces a real image of the scattering volume relocated in space (at P1), and finally the diaphragm D1 allows the adjustment of the optical aperture and as a consequence the spread of the $\vec{q}$-vectors around the main $\vec{q}$-direction. This real image can hence be placed away from mechanically disturbing components like thermostat windows and renders possible the optical

access to the real image of the scattering volume using a microscope objective lens (L3). The scanning of the scattering volume within the (x_1, x_2)-plane of the sample is provided either by tilting a thick glass plate around the z_3-axis (see figure 3.5) while keeping the sample position fixed, or by moving the sample along $\vec{z}_1$ and $\vec{z}_2$ using scanning stages while keeping the position of the scattering volume fixed (not shown in figure 3.5).

Magnification and spatial filtering of the real image are carried out in several consecutive steps using the lenses L3 till L5 and the adjustable spatial filters P1 to P3. The magnification is always achieved for the intermediate real images located at the pinholes and does not make use of a virtual image like the ocular of a usual microscope. The mirrors M1 and M2 and the lens L5 permit to map the remaining part of the originally illuminated scattering volume on the entrance pinhole P4 of the BRILLOUIN spectrometer.

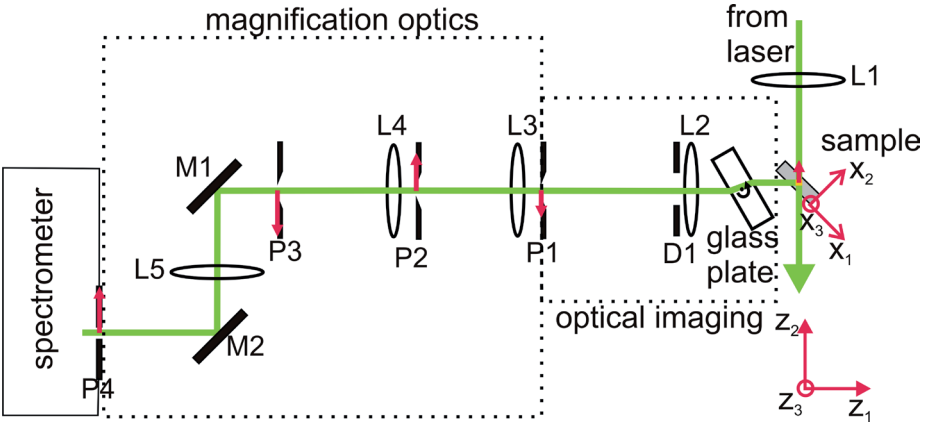

Fig. 3.5. Optical setup for high resolution $SBM^{\theta A}$. M: mirror, P: adjustable pinhole, L: lens, D: adjustable diaphragm. The red arrows denote the size and position of the imaged object, as well as those of the corresponding real images (maximal magnification factor of the whole optical setup: 150). $\{z_1, z_2, z_3\}$: laboratory coordinate system, $\{x_1, x_2, x_3\}$: sample coordinate system.

The adjustment of the optical components, which map the scattering volume to the pinhole P4, can be controlled by periscopes (not shown in figure 3.5). The more the diameter of the pinhole P1 is reduced, the smaller is the imaged scattering volume. Its selected diameter usually constitutes a compromise between a high spatial resolution and the amount of time needed for recording a reliable BRILLOUIN spectrum. The latter depends much on the scattering efficiency of the material within the scattering volume. The total optical setup can achieve a magnification factor of about 150, hence providing a spatial resolution of scattering volumes with lateral dimensions of about 1 µm (SANCTUARY *et al.* 2003). Similar to RAMAN microscopy, the depth of focus of the microscope system is an important factor. Keep in mind that the effective resolution of the BRILLOUIN microscope is not only limited by the optical setup but also by parameters like the optical homogeneity of the sample and the sample's surface roughness. Consequently, the effective resolution might be worse than 1 µm because of the sample's optical properties.

3.3.1 Selected scattering geometries for the SBM$^{\theta A}$ technique

As already suggested in section 3.2, in order to solve several specific physical problems by scanning BRILLOUIN microscopy, this technique must be employed in the θA scattering geometry rather than in backscattering. The θA scattering geometry shown in figure 3.6 is especially suited for probing the hypersonic properties of film- or plate-like samples. Note that in the following the scattering volume $V(\vec{r})$ usually remains fixed with respect to the laboratory coordinate system and that the sample is shifted and tilted in order to access its acoustic properties. Every point of the sample located in the (x_1, x_2)-plane can be reached by shifting the sample along the z_1-axis or the z_2-axis using scanning stages. Scanning the angle Φ by tilting the sample around the z_3-axis, which passes through the scattering volume, yields the angle-dependence of the hypersonic properties, i.e. the hypersonic velocity and attenuation indicatrices of the involved acoustic eigenmodes. This combination of two-dimensional scanning BRILLOUIN microscopy and angle-resolved BRILLOUIN spectroscopy allows generating a rather

complete acoustic image of even heterogeneous polycrystalline materials. The accessible information content consists in the grain size, the elastic anisotropy of the grains, and the elastic tensor components if the grains' symmetry is known. To conclude, this kind of angle-resolved hypersonic imaging gives a comprehensive picture about the hypersonic properties in dependence of the space and the orientation of the acoustic wave vector. These qualities of angle-resolved $SBM^{\theta A}$ are furthermore elucidated in chapter 4 using illustrative examples.

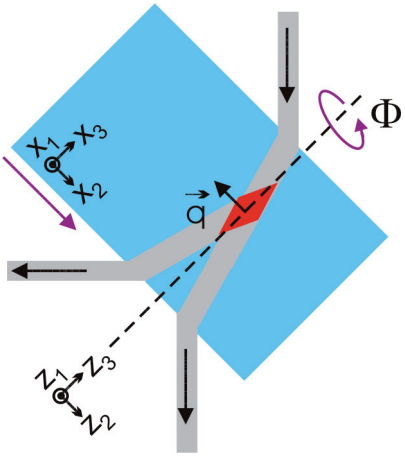

Fig. 3.6. Schematic representation of the sample arrangement for $SBM^{\theta A}$ investigations. Common scanning and tilt directions indicated by the magenta arrows. $\{x_1, x_2, x_3\}$: sample coordinate system, $\{z_1, z_2, z_3\}$: laboratory coordinate system, Φ : rotation angle around $\vec{z}_3$, $\vec{q}$: phonon wave vector.

Additional information, e.g. about acoustic dispersion, can be accessed by the reflection induced θA ($RI\theta A$) scattering geometry (KRÜGER *et al.* 1998, 2001) depicted in figure 3.7. The innovative nature of this optical setup consists in a mirror fixed at the backside of the film- or plate-like sample. The laser beam (1) incident on the sample under an angle of $\theta / 2$ is reflected by the mirror and exits the sample in direction (2). According to figure 3.7a, the collecting optics is adjusted in such a way that the scattering volume is focused on the reflected laser beam. Moreover, the

direction of the inelastically scattered light (3) is selected parallel to the incident beam. By these means the θA -scattering geometry is realized, yielding a phonon wave vector $q^{\theta A}(\vec{r})$ lying precisely parallel to the mirror's plane. The position of the scattering volume can easily be shifted along the reflected laser beam (KRÜGER *et al.* 1998, 2001): the necessary parallel shift of the beam (3) can be performed by putting a thick glass plate into the beam (3) and tilting it around an axis passing through it being parallel to $\vec{z}_1$, while keeping the sample's position fixed. This enables $SBM^{\theta A}$ investigations along the scattered beam (2) within the sample i.e. almost parallel to $\vec{x}_3$, in addition to the scanning in the x_1 and x_2 directions.

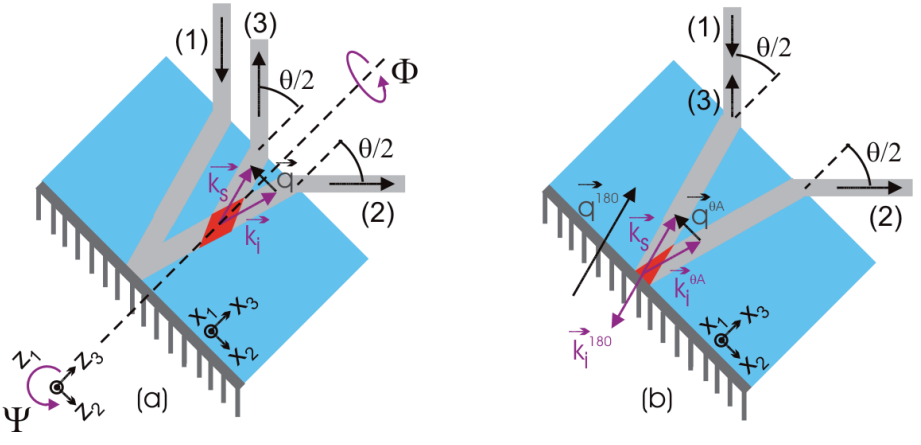

Fig. 3.7. Representation of (a) pure reflection induced θA (RIθA) scattering geometry, (b) combined RIθA *and backscattering geometry,* $\vec{k}_s$ *represents the scattered wave vector for both scattering geometries.* $\vec{k}_i$, $\vec{k}_s$ *: incident and scattered wave vector,* $\vec{q}$ *: wave vector of the acoustic phonon. Sample in blue, scattering volume in red. (1) laser beam incident on the sample, (2) laser beam leaving the sample, (3) selected direction of the inelastically scattered light emerging from the scattering volume.* $\{x_1, x_2, x_3\}$*: sample coordinate system,* $\{z_1, z_2, z_3\}$*: laboratory coordinate system .* Ψ*: angle of rotation around* $\vec{z}_1$, Φ*: angle of rotation around* $\vec{z}_3$.

Angle resolved $SBM^{\theta A}$ can easily be performed in the (x_1, x_2)-plane by scanning the angle Φ by tilting the sample around the z_3-axis while keeping the position of the scattering volume fixed. Prior to the invention of the $RI\theta A$ scattering geometry, the determination of acoustic dispersion for anisotropic materials had always been a huge challenge as the inner scattering angle within the sample had to be precisely adjusted and measured. The classical way to attack this problem was to prepare sample-cuts with surfaces suitable for an orthogonal entrance of the laser beam and for an exit of the scattered light beam orthogonal to the exit sample surface. By this means deviations between the inner and outer scattering angle were avoided. The $RI\theta A$ scattering arrangement given in figure 3.7 eliminates all of these difficulties and the related pitfalls.

The $RI\theta A$ scattering geometry furthermore allows for the first time for varying continuously the norm of the scattering vector $\vec{q}^{\theta A}(\vec{r})$ while maintaining its direction: the sample just needs to be tilted around the $\vec{z}_1$-axis by a continuous scan of the angle Ψ. Finally, the combination of spatially scanning $SBM^{\theta A}$ with Φ-scanning and Ψ-scanning permits an almost complete acoustic mapping of heterogeneous and inhomogeneous transparent samples.

The scattering geometry shown in figure 3.7b is a special case of that indicated in figure 3.7a; the scattering volume is just positioned in close vicinity to the mirror within the sample. For this optical arrangement, the sample's sound properties are determined simultaneously in the θA and the backscattering geometry. Note that for films with thicknesses identical or smaller than the lateral dimension of the scattering volume, i.e. typically some microns, this combined scattering geometry is automatically employed. For isotropic samples, it permits to determine the opto-acoustic dispersion function D^{180} of the scattering volume (KRÜGER 1989, KRÜGER *et al.* 1998), according to:

$$D^{180} = \frac{v^{180}}{v^{\theta A}} = \frac{f^{180}}{f^{\theta A} \cdot \sin(\theta/2)}. \qquad (3.2)$$

If no acoustic dispersion exists, the opto-acoustic dispersion function is equal to the refractive index of the material positioned within the scattering volume.